Journal of Sound and Vibration (1989) 134(1), 1-16

VIBRATIONS OF UNSYMMETRICALLY LAMINATED PLATES ANALYZED BY USING A HIGHER ORDER THEORY WITH A C° FINITE ELEMENT FORMULATION

T. KANT AND MALLIKARJUNA

Department of Civil Engineering, Indian Institute of Technology, Powai, Bombay 400 076, *India*

(*Received* 6 *June* 1988, *and in revised form* 19 *September* 1988)

Recently developed shear deformation theory is used to analyze vibrations of laminated composite and sandwich plates in conjunction with a C° isoparametric finite element formulation. The present theory is based on a higher order displacement model and the three-dimensional Hooke's laws for plate material, giving rise to a more realistic representation of the cross-sectional deformation. The theory does not require the usual shear correction coefficients generally associated with Reissner-Mindlin theories. A special mass lumping procedure is used in the dynamic equilibrium equations. The numerical examples presented are compared with 3-D elasticity/analytical and Mindlin's plate solutions, and it is demonstrated that the present model predicts the frequencies more accurately when compared with the first order shear deformation theories and classical plate theories.

1. INTRODUCTION

Multilayered composites have found wide use in many weight-sensitive structures such as aircraft and missile structural components, where high strength-to-weight and stiffness-to-weight ratios are required. A laminate is a multilayered composite made up of several individual layers (laminae), in each of which the fibres are oriented in a predetermined direction to provide efficiently the required strength and stiffness parameters. The finite element formulation provides a convenient method of solution for such laminated composites having complex geometry and arbitrary loading. In classical thin plate theory one assumes that the transverse normals to the mid-surface remain straight and normal to it during deformation, implying that the transverse shear deformation effects are negligible. As a result the free vibration frequencies calculated by using the thin plate theory are higher than those obtained by the Mindlin plate theory [1], in which transverse shear and rotary inertia effects are included; the deviation increases with increasing mode numbers. A reliable prediction of the response characteristics of composite and sandwich plates requires the use of shear deformable theories.

A great variety of shear deformation theories have been proposed to date and some are reviewed in reference [2]. They range from the first such theory by Stavsky [3] for laminated isotropic plates, through the theory of Yang, Norris and Stavsky [4] for laminated anisotropic plates, to various effective stiffness theories such as those discussed by Sun and Whitney [5], the Whitney and Sun higher order theory [6], and the 3-D elasticity theory approach of Srinivas *et al.* [7, 8] and Noor [9]. It has been shown by various investigators [2, 5-8] that the Yang-Norris-Stavsky (YNS) theory was adequate for predicting the flexural vibration response of laminated anisotropic plates in the first few modes. Whitney and Pagano [10] employed the YNS theory to study the free vibration of antisymmetric angle-ply plate strips (see also references [11, 12]). Bert and Chen [13]

0022-460X/89/190001+16 $03.00/0 © 1989 Academic Press Limited

presented a closed form solution for the free vibration of simply supported rectangular plates of antisymmetric angle-ply laminates. In the finite element vibration analysis, only limited investigations of laminated anisotropic plates can be found in the literature [14-18].

In recent years many refined plate theories have been presented to improve the predictions of laminate static [19-24] and dynamic [25-31] behaviour. The present paper attempts to provide a refined higher order plate model with a simple C^0 finite element formulation for free vibration of anisotropic laminated plates.

2. GOVERNING EQUATIONS

The elasticity solutions indicate that the transverse shear stresses vary parabolically through the plate thickness. This requires the use of a displacement field in which the in-plane displacements are expanded as cubic functions of the thickness co-ordinate. The consideration of normal stress in the thickness direction requires the transverse displacement also to be expanded as a function of the thickness co-ordinate. The polynomial expansion for transverse displacement is truncated at one order lower than the expansion for in-plane displacements such that the contributions to the transverse shear strains from in-plane displacements are of the same order in the thickness co-ordinate as that from the transverse displacement. The displacement field, which satisfies the above criteria is of the form

$$\begin{aligned} u(x,y,z,t) &= u_0(x,y,t) + z\theta_x(x,y,t) + z^2 u_0^*(x,y,t) + z^3\theta_x^*(x,y,t), \\ v(x,y,z,t) &= v_0(x,y,t) + z\theta_y(x,y,t) + z^2 v_0^*(x,y,t) + z^3\theta_y^*(x,y,t), \\ w(x,y,z,t) &= w_0(x,y,t) + z\theta_z(x,y,t) + z^2 w_0^*(x,y,t), \end{aligned} \tag{1}$$

where t is the time, u, v, w are the displacements of a generic point in the x, y, z directions respectively, u_0, v_0, w_0 are the associated mid-plane displacements, θ_x and θ_y are the rotations of the transverse normal in the x-z and y-z planes, u_0^*, v_0^*, w_0^*, θ_x^*, θ_y^* and θ_z are the corresponding higher order terms in the Taylor series expansion.

The strains associated with the displacements in equation (1) are

$$\begin{aligned} \varepsilon_x &= \partial u_0/\partial x + z\,\partial\theta_x/\partial x + z^2\,\partial u_0^*/\partial x + z^3\,\partial\theta_x^*/\partial x, \\ \varepsilon_y &= \partial v_0/\partial y + z\,\partial\theta_y/\partial y + z^2\,\partial v_0^*/\partial y + z^3\,\partial\theta_y^*/\partial y, \qquad \varepsilon_z = \theta_z + 2zw_0^*, \\ \gamma_{xy} &= (\partial u_0/\partial y + \partial v_0/\partial x) + z(\partial\theta_x/\partial y + \partial\theta_y/\partial x) + z^2(\partial u_0^*/\partial y + \partial v_0^*/\partial x) \\ &\quad + z^3(\partial\theta_x^*/\partial y + \partial\theta_y^*/\partial x), \\ \gamma_{yz} &= (\theta_y + \partial w_0/\partial y) + z(2v_0^* + \partial\theta_z/\partial y) + z^2(3\theta_y^* + \partial w_0^*/\partial y), \\ \gamma_{xz} &= (\theta_x + \partial w_0/\partial x) + z(2u_0^* + \partial\theta_z/\partial x) + z^2(3\theta_x^* + \partial w_0^*/\partial x). \end{aligned} \tag{2}$$

The stress-strain relation for the Lth lamina in the laminate co-ordinates (x, y, z) are written in a compacted form as

$$\boldsymbol{\sigma} = \underset{\sim}{Q}\boldsymbol{\varepsilon}. \tag{3a}$$

The transformed reduced stiffness matrix $\underset{\sim}{Q}$ with reference to plate axes (x, y, z) is obtained from the stiffness matrix $\underset{\sim}{C}$ with reference to fibre axes $(1, 2, 3)$ by using the coordinate transformation matrix $\underset{\sim}{T}$ from the relation [32],

$$\underset{\sim}{Q} = \underset{\sim}{T}^{-1}\underset{\sim}{C}[\underset{\sim}{T}^{-1}]^{\mathrm{T}} \tag{3b}$$

in which

$$\boldsymbol{\sigma}_{1\text{-}2\text{-}3} = \underset{\sim}{T}\boldsymbol{\sigma}_{x,y,z}, \qquad \underset{\sim}{Q} = \begin{bmatrix} Q_{ij} & \underset{\sim}{0} \\ \underset{\sim}{0} & Q_{lm} \end{bmatrix}, \quad \begin{Bmatrix} i, j = 1, 2, 3, 4 \\ l, m = 5, 6 \end{Bmatrix}, \tag{3c, d}$$

$$\boldsymbol{\sigma} = [\sigma_x, \sigma_y, \sigma_z, \tau_{xy}, \tau_{yz}, \tau_{xz}]^{\mathrm{T}}, \qquad \boldsymbol{\varepsilon} = [\varepsilon_x, \varepsilon_y, \varepsilon_z, \gamma_{xy}, \gamma_{yz}, \gamma_{xz}]^{\mathrm{T}}, \tag{3e, f}$$

these latter being the stress and strain vectors respectively with reference to the plate axes (x, y, z) (see Figure 1).

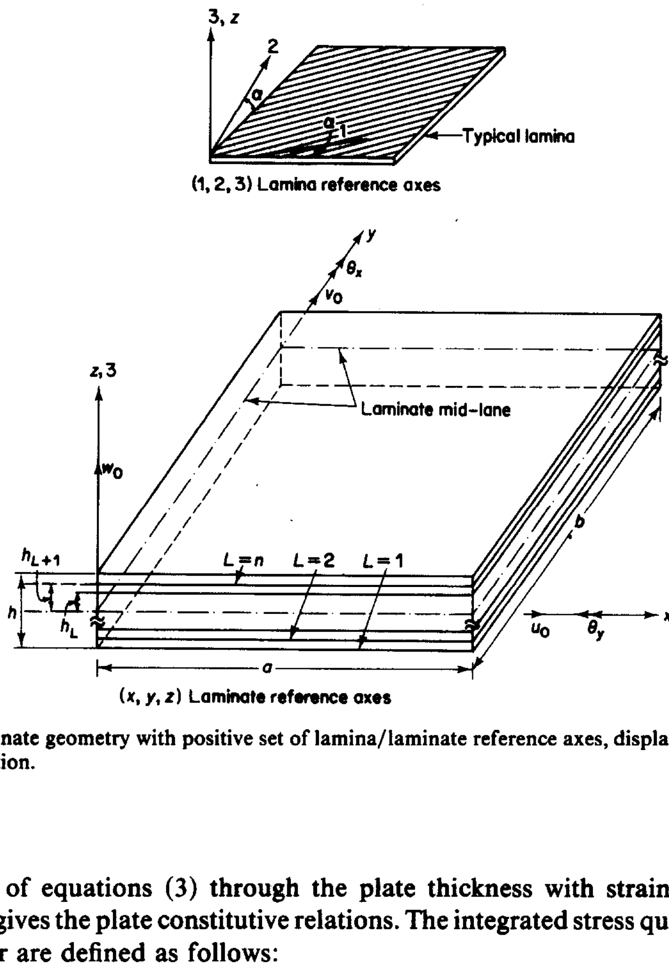

Figure 1. Laminate geometry with positive set of lamina/laminate reference axes, displacement components, and fibre orientation.

Integration of equations (3) through the plate thickness with strain terms given by equations (2) gives the plate constitutive relations. The integrated stress quantities obtained in this manner are defined as follows:

$$\begin{bmatrix} N_x & M_x & N_x^* & M_x^* \\ N_y & M_y & N_y^* & M_y^* \\ N_{xy} & M_{xy} & N_{xy}^* & M_{xy}^* \end{bmatrix} = \sum_{L=1}^{n} \int_{h_L}^{h_{L+1}} \begin{bmatrix} \sigma_x \\ \sigma_y \\ \tau_{xy} \end{bmatrix} [1, z, z^2, z^3] \, \mathrm{d}z, \tag{4a}$$

$$[N_z, M_z] = \sum_{L=1}^{n} \int_{h_L}^{h_{L+1}} [\sigma_z, z\sigma_z] \, \mathrm{d}z, \qquad \begin{bmatrix} Q_x & S_x & Q_x^* \\ Q_y & S_y & Q_y^* \end{bmatrix} = \sum_{L=1}^{n} \int_{h_L}^{h_{L+1}} \begin{bmatrix} \tau_{xz} \\ \tau_{yz} \end{bmatrix} [1, z, z^2] \, \mathrm{d}z. \tag{4b, c}$$

After integration, these can be written in matrix form as

$$\begin{bmatrix} \mathbf{N} \\ \mathbf{N}^* \\ \hline \mathbf{M} \\ \mathbf{M}^* \\ \hline \mathbf{Q} \\ \mathbf{Q}^* \end{bmatrix} = \left[\begin{array}{c|c|c} \underset{\sim}{D}_m & \underset{\sim}{D}_c & \underset{\sim}{0} \\ \hline \underset{\sim}{D}_c^{\mathrm{T}} & \underset{\sim}{D}_b & \underset{\sim}{0} \\ \hline \underset{\sim}{0} & \underset{\sim}{0} & \underset{\sim}{D}_s \end{array}\right] \begin{bmatrix} \boldsymbol{\varepsilon}_0 \\ \boldsymbol{\varepsilon}_0^* \\ \boldsymbol{\chi} \\ \boldsymbol{\chi}^* \\ \boldsymbol{\phi} \\ \boldsymbol{\phi}^* \end{bmatrix}, \quad \text{or } \bar{\boldsymbol{\sigma}} = \underset{\sim}{D}\bar{\boldsymbol{\varepsilon}}, \tag{5a, b}$$

where

$$\mathbf{N} = [N_x, N_y, N_{xy}]^{\mathrm{T}}, \quad \mathbf{N}^* = [N_x^*, N_y^*, N_{xy}^*, N_z]^{\mathrm{T}}, \quad \mathbf{M} = [M_x, M_y, M_{xy}]^{\mathrm{T}},$$

$$\mathbf{M}^* = [M_x^*, M_y^*, M_{xy}^*, M_z]^{\mathrm{T}}, \quad \mathbf{Q} = [Q_x, Q_y]^{\mathrm{T}}, \quad \mathbf{Q}^* = [S_x, S_y, Q_x^*, Q_y^*]^{\mathrm{T}},$$

$$\boldsymbol{\varepsilon}_0 = [\partial u_0/\partial x, \partial v_0/\partial y, \partial u_0/\partial y + \partial v_0/\partial x]^{\mathrm{T}}, \quad \boldsymbol{\varepsilon}_0^* = [\partial u_0^*/\partial x, \partial v_0^*/\partial y, \partial u_0^*/\partial y + \partial v_0^*/\partial x, \theta_z]^{\mathrm{T}},$$

$$\boldsymbol{\chi} = [\partial \theta_x/\partial x, \partial \theta_y/\partial y, \partial \theta_x/\partial y + \partial \theta_y/\partial x]^{\mathrm{T}}, \quad \boldsymbol{\chi}^* = [\partial \theta_x^*/\partial x, \partial \theta_y^*/\partial y, \partial \theta_x^*/\partial y + \partial \theta_y^*/\partial x, 2w_0^*]^{\mathrm{T}},$$

$$\boldsymbol{\varphi} = [\theta_x + \partial w_0/\partial x, \theta_y + \partial w_0/\partial y]^{\mathrm{T}},$$

$$\boldsymbol{\varphi}^* = [2u_0^* + \partial \theta_z/\partial x, 2v_0^* + \partial \theta_z/\partial y, 3\theta_x^* + \partial w_0^*/\partial x, 3\theta_y^* + \partial w_0^*/\partial y]^{\mathrm{T}}. \tag{5c}$$

The rigidity matrices $\underset{\sim}{D}_m$, $\underset{\sim}{D}_c$, $\underset{\sim}{D}_b$ and $\underset{\sim}{D}_s$ are given in Appendix A.

3. EQUATIONS OF MOTION AND ELEMENT MATRICES

Hamilton's principle and Lagrange's equations form the cornerstone of variational principles in mechanics. Here the time t is the independent variable and the integrand of the functional to be minimized is $KE - \Pi$ for a conservative force field where KE and Π are kinetic and potential energies, respectively. The integral $\int_{t_1}^{t_2} (KE - \Pi)\,\mathrm{d}t$ will have a stationary value when the variation of the integral is zero: i.e.,

$$\delta \int_{t_1}^{t_2} (KE - \Pi)\,\mathrm{d}t = 0. \tag{6a}$$

This constitutes Hamilton's principle. As might be expected on physical grounds, the solution of the variational problem of equation (6) represents a true minimum.

From Hamilton's principle one can derive Lagrange's equations. If $\mathbf{d}_i$ represents R independent degrees of freedom of a dynamical system, then in general

$$KE = KE(\mathbf{d}_r, \dot{\mathbf{d}}_r) \quad \text{and} \quad \Pi = \Pi(\mathbf{d}_r), \qquad r = 1, 2, \ldots, R. \tag{6b}$$

The Lagrangian function F of equation (6a) is then given by

$$F(t, \mathbf{d}_r, \dot{\mathbf{d}}_r) = KE(\mathbf{d}_r, \dot{\mathbf{d}}_r) - \Pi(\mathbf{d}_r). \tag{6c}$$

The Lagrange equations for a conservative system are then

$$\frac{\mathrm{d}}{\mathrm{d}t}\left(\frac{\partial F}{\partial \dot{\mathbf{d}}_r}\right) - \frac{\partial F}{\partial \mathbf{d}_r} = 0, \qquad r = 1, 2, \ldots, R. \tag{7}$$

The energies KE and Π are often easy to express, so that equation (7) is useful for obtaining the equation of motion for actual physical systems.

Since primary interest here is in the free vibration analysis, the potential energy due to the applied loads is zero. With the finite element method for the discretization of space, Lagrange's equations of motion, when placed in matrix form, become

$$\underline{M}\ddot{\mathbf{d}} + \underline{K}\mathbf{d} = \mathbf{0}, \tag{8}$$

where $\underline{K}$ and $\underline{M}$ are the global stiffness and mass matrices respectively, obtained by the assembly of the corresponding element matrices, and $\ddot{\mathbf{d}}$ is the second derivative of the displacements of the structure with respect to time.

The matrix equation (8) governing free vibration may be expressed as

$$\underline{K}\bar{\mathbf{d}} - \omega^2 \underline{M}\bar{\mathbf{d}} = \mathbf{0}, \tag{9}$$

where $\bar{\mathbf{d}}$ is a set of constant values at the nodes and is called the modal vector, and ω is the natural frequency of free vibration of the system. Equation (9) can be solved, after imposing the boundary conditions of the problem, by any standard eigenvalue program. For the purpose of evaluation, relation (9) is converted into the standard eigenvalue format.

$$(\underline{K} - \lambda \underline{M})\bar{\mathbf{d}} = \mathbf{0}, \qquad \lambda = \omega^2, \tag{10}$$

and the subspace iteration method [33] is used here to obtain the eigenvalues λ and the associated eigenvectors $\bar{\mathbf{d}}$.

4. ELEMENT MASS MATRIX

A special mass matrix diagonalization scheme that is more sophisticated than a lumped mass matrix is used here. The details of the scheme are discussed elsewhere [34]. The element mass matrix $\underline{M}^e$ is given by

$$\underline{M}^e = \int_A \underline{N}^{\mathrm{T}} \underline{m} \underline{N} \, \mathrm{d}(\text{Area}), \qquad \underline{N} = [N_1, N_2, \ldots, N_{NN}], \tag{11a, b}$$

in which NN is the number of nodes per element, and

$$\underline{m} = \left[\begin{array}{ccc|ccc|ccccc}
I_1 & & \underline{0} & & & & & & & & \\
 & I_1 & & & \underline{0} & & & & \underline{0} & & \\
\underline{0} & & I_1 & & & & & & & & \\
\hline
 & & & I_2 & & \underline{0} & & & & & \\
 & \underline{0} & & & I_2 & & & & \underline{0} & & \\
 & & & \underline{0} & & I_2 & & & & & \\
\hline
 & & & & & & I_3 & & & & \\
 & & & & & & & I_3 & & \underline{0} & \\
 & \underline{0} & & & \underline{0} & & & & I_3 & & \\
 & & & & & & & \underline{0} & & I_4 & \\
 & & & & & & & & & & I_4
\end{array}\right], \tag{11c}$$

in which I_1, I_2 and I_3, I_4 are normal inertia, rotary inertia and higher order inertias, respectively.

They are given by

$$[I_1, I_2, I_3, I_4] = \sum_{L=1}^{n} \int_{h_L}^{h_{L+1}} [1, z^2, z^4, z^6] \rho^L \, \mathrm{d}z, \tag{11d}$$

where ρ^L is the material density of the Lth layer.

5. ELEMENT STIFFNESS MATRIX

The domain Ω is decomposed into a set of finite elements. The restriction of the Lagrangian functional F to the finite element Ω_e is denoted by F_e: i.e.,

$$F = \sum_{e=1}^{NE} F_e(u_0, v_0, w_0, \theta_x, \theta_y, \theta_z, u_0^*, v_0^*, w_0^*, \theta_x^*, \theta_y^*), \tag{12}$$

where NE denotes the total number of finite elements in the mesh. In C^0 finite element theory, the continuum displacement vector within the element is discretized such that

$$\boldsymbol{\delta} = \sum_{i=1}^{NN} N_i \boldsymbol{\delta}_i, \tag{13}$$

in which NN is the number of nodes in an element, N_i is the simple isoparametric interpolating (shape) function associated with node i in terms of the normalized co-ordinates ξ and η, and $\boldsymbol{\delta}_i$ is the generalized displacement vector corresponding to the ith node of an element. The generalized strain $\bar{\boldsymbol{\varepsilon}}$ at any point within an element can be expressed by the relationship

$$\bar{\boldsymbol{\varepsilon}} = \sum_{i=1}^{NN} \underline{B}_i \boldsymbol{\delta}_i, \tag{14a}$$

where

$$\begin{aligned}\bar{\boldsymbol{\varepsilon}} = \Bigg[& \frac{\partial u_0}{\partial x}, \frac{\partial v_0}{\partial y}, \frac{\partial u_0}{\partial y} + \frac{\partial v_0}{\partial x}, \frac{\partial u_0^*}{\partial x}, \frac{\partial v_0^*}{\partial y}, \frac{\partial u_0^*}{\partial y} + \frac{\partial v_0^*}{\partial x}, \\ & \theta_z, \frac{\partial \theta_x}{\partial x}, \frac{\partial \theta_y}{\partial y}, \frac{\partial \theta_x}{\partial y} + \frac{\partial \theta_y}{\partial x}, \frac{\partial \theta_x^*}{\partial x}, \frac{\partial \theta_y^*}{\partial y}, \\ & \frac{\partial \theta_x^*}{\partial y} + \frac{\partial \theta_y^*}{\partial x}, 2w_0^*, \theta_x + \frac{\partial w_0}{\partial x}, \theta_y + \frac{\partial w_0}{\partial y}, 2u_0^* + \frac{\partial \theta_z}{\partial x}, \\ & 2v_0^* + \frac{\partial \theta_z}{\partial y}, 3\theta_x^* + \frac{\partial w_0^*}{\partial x}, 3\theta_y^* + \frac{\partial w_0^*}{\partial y} \Bigg]^{\mathrm{T}},\end{aligned} \tag{14b}$$

$$\boldsymbol{\delta}_i = [u_{0i}, v_{0i}, w_{0i}, \theta_{xi}, \theta_{yi}, \theta_{zi}, u_{0i}^*, v_{0i}^*, w_{0i}^*, \theta_{xi}^*, \theta_{yi}^*]^{\mathrm{T}}. \tag{14c}$$

The non-zero terms in the strain displacement matrix $\underline{B}_i$ are as follows:

$$\begin{gathered} B_{1,1} = B_{3,2} = B_{4,7} = B_{6,8} = B_{8,4} = B_{10,5} = B_{11,10} = B_{13,11} = B_{15,3} = B_{17,6} = B_{19,9} = \partial N_i/\partial x, \\ B_{2,2} = B_{3,1} = B_{5,8} = B_{6,7} = B_{9,5} = B_{10,4}, B_{12,11} = B_{13,10} = B_{16,3} = B_{18,6} = B_{20,9} = \partial N_i/\partial y, \\ B_{14,9} = B_{17,7} = B_{18,8} = 2N_i, \quad B_{7,6} = B_{15,4} = B_{16,5} = N_i, \quad B_{19,10} = B_{20,11} = 3N_i. \end{gathered} \tag{14d}$$

It can be observed that for a symmetric laminate the submatrices $\underline{D}_m$ and $\underline{D}_c$ vanish in equations (5a) indicating that there will not be any coupling between membrane and bending stress resultants. Upon evaluating the matrices $\underline{D}$ and $\underline{B}$ as given by equations (5) and (14), respectively, the element stiffness matrix can be readily computed by using the standard relation,

$$K_{ij}^e = \int_{-1}^{+1} \int_{-1}^{+1} \underline{B}_i^{\mathrm{T}} \underline{D} \underline{B}_j |\underline{J}| \, \mathrm{d}\xi \, \mathrm{d}\eta, \tag{15}$$

where $|J|$ is the determinant of the Jacobian matrix.

The computation of the element stiffness matrix is economized by explicit multiplication of the $\underset{\sim}{B}_i^{\mathrm{T}}$, $\underset{\sim}{D}$ and $\underset{\sim}{B}_j$ matrices instead of carrying out the full matrix multiplication of the triple product. Due to symmetry of the stiffness matrix, only blocks lying on one side of the main diagonal are formed [35].

6. DISCUSSION OF THE NUMERICAL RESULTS

Numerical computations were carried out for the free undamped transverse vibration analysis of laminated anisotropic plates. The effects of material anisotropy, transverse shear deformation, the ratio of span-to-thickness, coupling between stretching and bending and the number of laminae in the laminate on the frequencies are investigated. For all the numerical examples, a full plate was discretized with a 4×4 mesh of the nine-noded Lagrangian quadrilateral elements. The selective integration scheme based on Gauss quadrature rules, viz., 3×3 for membrane, coupling, flexure and inertia terms and 2×2 for shear term contributions, was employed. All the computations were carried out on CYBER 180/840 computer in single precision. The boundary conditions used for the simply supported plates are of two types, viz., (a) cross-ply boundary condition (WSS1),

$$v_0 = w_0 = \theta_y = \theta_z = v_0^* = w_0^* = \theta_y^* = 0 \qquad \text{at } x = 0, a,$$

$$u_0 = w_0 = \theta_x = \theta_z = u_0^* = w_0^* = \theta_x^* = 0 \qquad \text{at } y = 0, b;$$

(b) angle-play boundary conditions (WSS2)

$$u_0 = w_0 = \theta_y = \theta_z = u_0^* = w_0^* = \theta_y^* = 0 \qquad \text{at } x = 0, a,$$

$$v_0 = w_0 = \theta_x = \theta_z = v_0^* = w_0^* = \theta_x^* = 0 \qquad \text{at } y = 0, b.$$

For a clamped plate (WCC), all the 11 degrees of freedom

$$(u_0, v_0, w_0, \theta_x, \theta_y, \theta_z, u_0^*, v_0^*, w_0^*, \theta_x^*, \theta_y^*)$$

are restrained at $x = 0$, a and $y = 0$, b.

In order to establish the versatility of the present higher order shear deformation theory in its ability to model both thick and thin composite and sandwich plates, two computer programs PHOST11 (Program for Higher Order Shear deformation Theory with 11 degrees of freedom) and PHOST6 (Program for Higher Order Shear deformation Theory with six degrees of freedom) were developed separately. PHOST6 was developed particularly to analyze only symmetric laminates. The preliminary results of isotropic, orthotropic and symmetric laminates were presented in reference [36]. In addition to the PHOST11 and PHOST6 programs, the PFOST5 (Program for First Order Shear deformation Theory with five degrees of freedom, i.e., Mindlin–Reissner theory) was also developed to validate and verify the present PHOST11 particularly for composite-sandwich plates.

A bidirectional square laminate as shown in Figure 1 was considered for numerical evaluations. The material elastic characteristics of the individual layers were taken to be those of high fibrous composites (typical graphite/epoxy) as characterized by Material 1 given in Table 1. The values of E_2 and ρ are arbitrary because of the non-dimensionalization used (set to unity here). Table 2 shows the effects of degree of orthotropy of the individual layers on the fundamental frequency of simply supported square multilayered composite plates with $a/h = 5$. The ratio of E_1/E_2 was varied between 3 and 40 and the number of layers were varied between 2 and 10. The present PHOST11 results are compared with the available 3-D elasticity solution [9]. The agreement is seen to be excellent. It is seen that the fundamental frequency increases with the increase in number of layers and/or increase of degree of orthotropy. For antisymmetrically laminated plates, as the

TABLE 1

Material properties

Description	Elastic properties
Material 1 (non-dimensional typical graphite/epoxy)	$E_1/E_2 = 40$, $E_3/E_2 = 1$, $G_{12}/E_2 = G_{13}/E_2 = 0{\cdot}6$, $G_{23}/E_2 = 0{\cdot}5$, $\upsilon_{12} = \upsilon_{23} = \upsilon_{13} = 0{\cdot}25$, $\rho = 1$
Material 2 (top and bottom stiff layers made of graphite/epoxy prepreg system and core is of U.S. commercial aluminium honeycomb 1/4 inch cell size, 0·003 inch foil)	Face sheet: $E_1 = 1{\cdot}308 \times 10^7\ N/\text{cm}^2$, $E_2 = E_3 = 1{\cdot}06 \times 10^6\ N/\text{cm}^2$ $G_{12} = G_{13} = 6{\cdot}0 \times 10^5\ N/\text{cm}^2$, $G_{23} = 3{\cdot}9 \times 10^5\ N/\text{cm}^2$ $\rho = 1{\cdot}58 \times 10^{-5}\ N s^2/\text{cm}^4$, $\nu_{12} = \nu_{13} = 0{\cdot}28$, $\nu_{23} = 0{\cdot}34$ thickness of each top stiff layer = 0·025 h thickness of each bottom stiff layer = 0·08125 h Core: $G_{23} = 1{\cdot}772 \times 10^4\ N/\text{cm}^2$, $G_{13} = 5{\cdot}206 \times 10^4\ N/\text{cm}^2$ $\rho = 1{\cdot}009 \times 10^{-6}\ N s^2/\text{cm}^4$ thickness of core = 0·6 h

TABLE 2

Effect of number of layers and degree of orthotropy of individual layers on the fundamental frequency of simply supported square multilayered composite plates with $a/h = 5$, $\bar{\omega} = \omega(\rho h^2/E_2)^{1/2}$, Material 1 (WSS1)

No. of layers	Source	E_1/E_2				
		3	10	20	30	40
2	3-D elasticity theory [9]	0·25031	0·27938	0·30698	0·32705	0·34250
	Present PHOST11	0·24782 (−0·99)	0·27764 (−0·62)	0·30737 (+0·12)	0·33003 (+0·91)	0·34810 (+1·633)
	Present PFOST5	0·24829 (−0·80)	0·27751 (−0·67)	0·30998 (+0·98)	0·33771 (+3·26)	0·35995 (+5·10)
	CPT	0·27082 (+8·19)	0·30968 (+10·84)	0·35422 (+15·38)	0·39335 (+20·27)	0·42884 (+25·21)
	Reddy [26]	0·24868 (−0·65)	0·27955 (−0·06)	0·31284 (+1·91)	0·34020 (+4·02)	0·36348 (+6·12)
4	3-D elasticity theory [9]	0·26182	0·32578	0·37622	0·40660	0·42719
	Present PHOST11	0·25997 (−0·70)	0·32486 (−0·28)	0·37801 (+0·47)	0·41041 (+0·93)	0·43240 (+1·21)
	Present PFOST5	0·26012 (−0·65)	0·32889 (+0·95)	0·38741 (+2·97)	0·42462 (+4·43)	0·45062 (+5·48)
	CPT	0·28676 (+9·52)	0·38877 (+19·33)	0·49907 (+32·65)	0·58900 (+44·86)	0·66690 (+56·11)
	Reddy [26]	0·26003 (−0·68)	0·32782 (+0·62)	0·38506 (+2·35)	0·42139 (+3·64)	0·44686 (+4·60)

TABLE 2—*continued.*

No. of layers	Source	E_1/E_2 3	10	20	30	40
6	3-D elasticity theory [9]	0·26440	0·33657	0·39359	0·42783	0·45091
	Present PHOST11	0·26194 (−0·93)	0·33423 (−0·69)	0·39249 (−0·27)	0·42766 (−0·04)	0·45141 (+0·11)
	Present PFOST5	0·26222 (−0·82)	0·33664 (+0·02)	0·39756 (+1·00)	0·43512 (+1·70)	0·46083 (+2·19)
	CPT	0·28966 (+9·55)	0·40215 (+19·48)	0·52234 (+32·71)	0·61963 (+44·83)	0·70359 (+56·03)
	Reddy [26]	0·26223 (−0·82)	0·33621 (−0·11)	0·39672 (+0·79)	0·43419 (+1·48)	0·46005 (+2·02)
10	3-D elasticity theory [9]	0·26583	0·34250	0·40337	0·44011	0·46498
	Present PHOST11	0·26331 (−0·94)	0·33989 (−0·76)	0·40069 (−0·66)	0·43780 (−0·52)	0·46295 (−0·43)
	Present PFOST5	0·26329 (−0·96)	0·34043 (−0·60)	0·40239 (−0·24)	0·44003 (−0·02)	0·46554 (+0·12)
	CPT	0·29115 (+9·52)	0·40888 (+19·38)	0·53397 (+32·37)	0·63489 (+44·25)	0·72184 (+55·24)
	Reddy [26]	0·26337 (−0·92)	0·34050 (−0·58)	0·40270 (−0·16)	0·44079 (+0·15)	0·46692 (+0·41)

Values in brackets give percentage errors with respect to the elasticity solution [9].

number of layers increased from two to four, the accuracy of the classical plate theory (CPT) sharply deteriorated. Further increase in the number of layers does not have a significant effect on the accuracy. The error in the CPT predictions was mainly due to the neglect of transverse shear deformation. The error in the predictions of PHOST11 did not exceed 1·6 percent even for the case of highly orthotropic thick laminate with $E_1/E_2=40$. The corresponding error estimate for PFOST5 and Reddy's exact (series) solution of a higher order theory [26] were seen to be 5·5 percent and 6·1 percent respectively. For small degrees of orthotropy ($E_1/E_2=3$–10), the difference in the finite element results of PHOST11 and PFOST5 and the exact (series) solution of a higher order theory of Reddy [26] is almost negligible.

To study the effect of side-thickness ratio on the non-dimensional fundamental frequencies (see Table 3), the results were obtained for the following cases with elastic properties corresponding to Material 1 given in Table 1: (i) two-layer, equal thickness, antisymmetric cross-ply (0°/90°) square laminate; (ii) two-layer, equal thickness, antisymmetric angle-ply (45°/−45°) square laminate; (iii) eight-layer, equal thickness, antisymmetric angle-ply (45°/−45°/45° · · ·) square laminate. The CPT solution included the rotary inertia effects [25]. The results of the present PHOST11 were close to the closed form solution (CFS) of a higher order theory [25] but, as seen in Table 2, the present theory gives more accurate results than the analytical (series) solution of the third order theory of Reddy

TABLE 3

Non-dimensionalized fundamental frequencies $\bar{\omega} = (\omega a^2/h)\sqrt{\rho/E_2}$ *of simply supported skew-symmetric angle-ply square plates, Material* 1

	2 layer (0°/90°) WSS1			2 layer (45°/−45°) WSS2			8 layer (45°/−45°/45° · · ·) WSS2		
a/h	Present PHOST11	CFS [25]	CPT	Present PHOST11	CFS [25]	CPT	Present PHOST11	CFS [25]	CPT
5	8·702	9·010	10·584	10·215	10·840	13·885	12·718	12·972	15·708
10	10·415	10·449	11·011	12·879	13·263	14·439	19·107	19·266	25·052
20	11·060	10·968	11·125	14·132	14·246	14·587	23·169	23·239	25·212
50	11·202	11·132	11·158	14·561	14·572	14·630	24·889	24·905	25·258
100	11·208	11·156	11·163	14·626	14·621	14·636	25·174	25·174	25·264

Values in brackets give percentage errors with respect to the closed form solution [25].

[25]. The CPT overestimates the frequencies. The effect of the coupling between bending and stretching on the fundamental frequencies of simply-supported cross-ply (0°/90°/ $\cdots$ 90°) and angle-ply (45°/ −45°/ $\cdots$ −45°) laminates (Material 1) with $a/h = 5$ is shown in Table 4. The six-degrees-of-freedom $(w_0, \theta_x, \theta_y, w_0^*, \theta_x^*, \theta_y^*)$ solution (PHOST6) which included bending action only was obtained by suppressing the in-plane displacement degrees of freedom $(u_0, v_0, \theta_z, u_0^*, v_0^*)$. As the a/h ratio increased the effect of the coupling between bending and stretching increased for two layers and four layers. The percentage errors were as high as 67 percent for cross-ply (0°/90°) and 75 percent for angle-ply (45°/ −45°). The percentage error decreased with the increase in number of layers. It was thus seen that the coupling between bending and stretching had a significant effect on the behaviour of antisymmetric laminates with few laminae.

Table 5 shows a comparison of non-dimensional frequencies, for a four-layer laminated square plate (45°/ −45°/45°/ −45°) with $a/h = 10$ obtained by various investigators. It includes the results of the present PHOST11 and PFOST5, CFS of Bert and Chen [13], finite element PFOST results of Reddy [18] and CPT estimates. The predictions of the present theories (PHOST11 and PFOST5) and CPT increased with increasing longitudinal and transverse wavenumbers (m and n). The results of the present PHOST11 and PFOST5 were very close to the CFS [13], whereas the PFOST finite element results with the 8-noded Serendipity element given by Reddy [18] were far away from the CFS [13] for higher modes. The discrepancies observed in Reddy's results could be due to his analyzing angle-ply laminate by discretizing only a quarter and/or a half plate. Since no mirror image of the cross-sectional plane of symmetry existed for angle-ply laminates, a full plate should be discretized for analysis.

Finally, a comparison of the effects of the mode numbers on the associated frequencies of a composite-sandwich plate (0°/45°/90°/core/90°/45°/30°/0°) as predicted by the present PHOST11 and PFOST5 was made and is shown in Table 6. Two different types of boundary conditions were used: simply supported and clamped. The elastic properties corresponding to Material 2 as given in Table 2 were used. The effect of the shear moduli G_{23} and G_{13} of stiff layers were seen to be more pronounced for thicker laminates. For a thick sandwich laminate, the difference between the frequencies from the two theories (PHOST11 and PFOST5) increased with increasing mode numbers. While the study reported here was concentrated on unsymmetric laminated plates, the theory presented and the computer programs developed are valid for general laminates with various edge conditions.

7. CONCLUSION

A refined higher order theory and the Mindlin–Reissner theory have been used for vibration analysis of unsymmetrically laminated square composite and sandwich plates. A C^0 continuous finite element model of the present higher-order theory is validated by comparisons with the available 3-D elasticity and closed form solutions. The present PHOST11 results are in excellent agreement with the 3-D elasticity solutations. This is due to a realistic representation of the cross-sectional deformation and consideration of the complete stress–strain law. The present PHOST11 does not require the usual shear correction coefficients generally associated with PFOST5 of Mindlin–Reisner. The simplifying assumptions made in CPT and PFOST5 are reflected by the high percentage error in the results of thick composite-sandwich plates. It is believed that the improved shear deformation theory presented here is essential for reliable analyses of sandwich-type laminated composite plates.

TABLE 4

Effect of the coupling between bending and stretching on the non-dimensional fundamental frequencies $\bar{\omega} = \omega\sqrt{\rho h^2/E_2}$ *of a simply supported square plate, Material* 1; CP = *cross-ply* (0°/90°/0° · · · 90°), AP = *angle-ply* (45°/ −45°/45°/ · · · −45°)

a/h	Lamination scheme and boundary conditions	2 layers PHOST11	2 layers PHOST6	4 layers PHOST11	4 layers PHOST6	6 layers PHOST11	6 layers PHOST6	10 layers PHOST11	10 layers PHOST6
5	CP(WSS1)	0·348106	0·469961 (+35·00)	0·432405	0·469961 (+8·68)	0·451414	0·469961 (+4·10)	0·462951	0·469961 (+1·51)
	AP(WSS2)	0·400602	0·523067 (+30·57)	0·477902	0·523067 (+9·45)	0·498825	0·523067 (+4·86)	0·513729	0·523067 (+1·81)
10	CP(WSS1)	0·104157	0·159299 (+52·94)	0·146309	0·159299 (+8·87)	0·153371	0·159299 (+3·86)	0·157158	0·159299 (+1·36)
	AP(WSS2)	0·128794	0·195608 (+51·87)	0·178639	0·195608 (+9·49)	0·187647	0·195608 (+4·24)	0·192685	0·195608 (+1·51)
20	CP(WSS1)	0·027651	0·044969 (+62·63)	0·041238	0·044969 (+9·05)	0·043329	0·044969 (+3·78)	0·044382	0·044969 (+1·32)
	AP(WSS2)	0·035329	0·059217 (+67·61)	0·054020	0·059217 (+9·62)	0·056912	0·059217 (4·05)	0·058388	0·059217 (+1·41)
50	CP(WSS1)	0·004507	0·007495 (+66·29)	0·006868	0·007495 (+9·13)	0·007222	0·007495 (+3·78)	0·007397	0·007495 (+1·32)
	AP(WSS2)	0·005824	0·010174 (+74·69)	0·009274	0·010174 (+9·70)	0·009782	0·010174 (+4·00)	0·010035	0·010174 (+1·38)
100	CP(WSS1)	0·001129	0·001885 (+66·96)	0·001727	0·001885 (+9·15)	0·001817	0·001885 (+3·74)	0·001861	0·001885 (+1·28)
	AP(WSS2)	0·001463	0·002572 (+75·80)	0·002344	0·002572 (+9·72)	0·002473	0·002572 (+4·00)	0·002537	0·002572 (+1·37)

Values in brackets give percentage deviation with respect to PHOST11.

TABLE 5

Dimensionless fundamental frequencies $\bar{\omega} = \omega a^2(\rho / E_2 h^2)^{1/2}$ for various longitudinal and transverse wave numbers (m and n) of a simply supported square plate ($a/h = 10$, Material 1, stacking sequence $45°/-45°/45°/-45°$, WSS2)

					Reddy [18]			
m	n	Present PHOST11	Present PFOST5	Bert and Chen [13]	Half plate 2×2 NDF = 5	Half plate 2×2 NDF = 3	Half plate 4×2 NDF = 3	CPT
1	1	17·86	18·45	18·46	18·259	19·244	19·153	23·53
1	2	34·46	34·54	34·87	35·585	36·512	35·405	53·74
2	2	48·97	49·99	50·52	—	—	—	94·11
1	3	53·21	53·87	54·27	54·367	55·727	55·390	98·87
2	3	65·52	65·08	67·17	70·315	70·895	67·637	147·65
1	4	77·39	75·25	75·58	79·315	79·882	76·412	160·35
3	3	83·52	81·99	82·84	99·597	100·012	84·725	211·75
2	4	87·27	85·05	85·27	—	—	—	214·97
1	5	99·74	98·46	97·56	108·665	109·792	105·057	238·72
3	4	101·93	99·45	99·02	—	182·255	109·292	288·76
2	5	—	102·22	104·95	—	226·432	116·385	297·30

TABLE 6

Comparison of natural frequencies ($\omega/2\pi$) *of a eight-layer* (0°/45°/90°/Core/90°/45°/30°/0°) *square composite-sandwich plate* (*Material* 2) $a = b = 100$ cm)

Modal no.	Considering G_{23} and G_{13} of stiff layers							
	Simply supported (WSS2)				Clamped (WCC)			
	$a/h = 10$		$a/h = 100$		$a/h = 10$		$a/h = 100$	
	PHOST11	PFOST5	PHOST11	PFOST5	PHOST11	PFOST5	PHOST11	PFOST5
1	464	516	59	59	641	754	103	102
2	853	1013	127	127	995	1244	192	192
3	943	1154	154	154	997	1382	231	231
4	956	1501	211	211	1053	1706	295	296
5	1002	1773	264	265	1161	1961	374	378
6	1201	1993	321	322	1385	2150	440	444
7	1226	2042	326	327	1399	2173	459	462
8	1245	2173	387	389	1429	2222	525	531

Modal no.	Neglecting G_{23} and G_{13} of stiff layers							
	Simply supported (WSS2)				Clamped (WCC)			
	$a/h = 10$		$a/h = 100$		$a/h = 10$		$a/h = 100$	
	PHOST11	PFOST5	PHOST11	PFOST5	PHOST11	PFOST5	PHOST11	PFOST5
1	281	297	57	58	321	332	94	98
2	431	430	120	123	456	446	168	176
3	530	579	142	150	580	586	194	216
4	582	582	192	201	597	595	245	268
5	603	656	236	243	621	666	302	314
6	628	673	279	297	641	674	346	374
7	638	678	282	309	673	680	375	411
8	665	744	327	357	678	750	396	432

ACKNOWLEDGMENTS

Partial support of this research by the Aeronautics Research and Development Board, Ministry of Defence, Government of India through its Grant No. Aero/RD-134/100/84-85/362 is gratefully acknowledged.

The authors are thankful to the reviewers for their extensive constructive comments and suggestions, which have been incorporated in this final version of the manuscript.

REFERENCES

1. R. D. MINDLIN 1951 *Journal of Applied Mechanics* **18**, 31–38. Influence of rotary inertia and shear on flexural motions of isotropic elastic plates.
2. C. W. BERT 1974 in *Structural Design and Analysis, Part* 1, (C. C. Chamis, editor). Chapter 4: Analysis of Plates. New York: Academic Press.
3. Y. STAVSKY 1965 in *Topics in Applied Mechanics* (D. Abir, F. Ollendorff and M. Reiner, editors), 105–?. New York: American Elsevier. On the theory of symmetrically heterogeneous plates having the same thickness variation of the elastic moduli.

4. P. C. YANG, C. H. NORRIS and Y. STAVSKY 1966 *International Journal of Solids and Structures* **2**, 665-684. Elastic wave propagation in heterogeneous plates.
5. C. T. SUN and J. M. WHITNEY 1973 *American Institute of Aeronautics and Astronautics Journal* **11**, 178-183. Theories for the dynamic response of laminated plates.
6. J. M. WHITNEY and C. T. SUN 1973 *Journal of Sound and Vibration* **30**, 85-97. A higher order theory for extensional motion of laminated composites.
7. S. SRINIVAS, C. V. JOGA RAO and A. K. RAO 1970 *Journal of Sound and Vibration* **12**, 187-199. An exact analysis for vibration of simply supported homogeneous and laminated thick rectangular plates.
8. S. SRINIVAS and A. K. RAO 1970 *International Journal of Solids and Structures* **6**, 1463-1481. Bending vibration and buckling of simply supported thick orthotropic rectangular plates and laminates.
9. A. K. NOOR 1973 *American Institute of Aeronautics and Astronautics Journal* **11**, 1038-1039. Free vibration of multilayered composite plates.
10. J. M. WHITNEY and N. J. PAGANO 1970 *Journal of Applied Mechanics* **37**, 1031-1036. Shear deformation in heterogeneous anisotropic plates.
11. R. C. FORTIER and J. N. ROSSETTOS 1973 *Journal of Applied Mechanics* **40**, 299-301. On the vibration of shear deformable curved anisotropic composite plates.
12. P. K. SINHA and A. K. RATH 1975 *Aeronautical Quarterly* **26**, 211-218. Vibration and buckling of cross-ply laminated circular cylindrical panels.
13. C. W. BERT and T. L. C. CHEN 1978 *International Journal of Solids and Structures* **14**, 465-473. Effect of shear deformation on vibration of antisymmetric angle-ply laminated rectangular plates.
14. A. K. NOOR and M. D. MATHERS 1976 *American Institute of Aeronautics and Astronautics Journal* **14**, 282-285. Anisotropy and shear deformation in laminated composite plates.
15. A. K. NOOR and M. D. MATHERS 1977 *International Journal for Numerical Methods in Engineering* **11**, 289-307. Finite element analysis of anisotropic plates.
16. E. HINTON 1976 *Earthquake Engineering and Structural Dynamics* **4**, 511-514. A note on a thick finite strip method for the free vibration of laminated plates (short communication).
17. E. HINTON 1976 *Earthquake Engineering and Structural Dynamics* **4**, 515-516. A note on a finite element method for the free vibrations of laminated plates (short communication).
18. J. N. REDDY 1979 *Journal of Sound and Vibration* **66**, 565-576. Free vibration of antisymmetric angle-ply laminated plates including transverse shear deformation by the finite element method.
19. T. KANT 1982 *Computer Methods in Applied Mechanics and Engineering* **31**, 1-18. Numerical analysis of thick plates.
20. T. KANT, D. R. J. OWEN and O. C. ZIENKIEWICZ 1982 *Computers and Structures* **15**, 177-183. A refined higher-order C^0 plate bending element.
21. J. N. REDDY 1984 *Journal of Applied Mechanics* **51**, 745-752. A simple higher-order theory for laminated composite plates.
22. B. N. PANDYA and T. KANT 1988 *Computer Methods in Applied Mechanics and Engineering* **66**, 173-198. Flexural analysis of laminated composites using refined higher-order C^0 plate bending elements.
23. B. N. PANDYA and T. KANT 1987 *Mechanics Research Communication* **14**, 107-113. A consistent refined theory for flexure of a symmetric laminate.
24. B. N. PANDYA and T. KANT 1988 *Computers and Structures* **28**, 119-133. A refined higher-order generally orthotropic C^0 plate bending element.
25. J. N. REDDY and N. D. PHAN 1985 *Journal of Sound and Vibration* **98**, 157-170. Stability and vibration of isotropic and laminated plates according to a higher-order shear deformation theory.
26. N. S. PUTCHA and J. N. REDDY 1986 *Journal of Sound and Vibration* **104**, 285-300. Stability and vibration analysis of laminated plates by using a mixed element based on a refined plate theory.
27. MALLIKARJUNA and T. KANT 1988 *Journal of Sound and Vibration* **126**, 463-475. Dynamics of laminated composite plates with a higher order theory and finite element discretization.
28. T. KANT, R. V. RAVICHANDRAN, B. N. PANDYA and MALLIKARJUNA 1988 *Composite Structures* **9**, 314-342. Finite element transient dynamic analysis of isotropic and fibre reinforced composite plates using a higher-order theory.
29. D. R. J. OWEN and Z. H. LI 1988 *Computers and Structures* **26**, 907-914. A refined analysis of laminated plates by finite element displacement methods, II: vibration and stability.
30. MALLIKARJUNA and T. KANT 1988 *Proceedings of Third International Conference on Recent Advances in Structural Dynamics*, 18-22 July 1988, *Southampton, U.K.* On transient response of laminated composite plates based on a higher order theory.

31. MALLIKARJUNA and T. KANT 1988 *American Society of Mechanical Engineers, Journal of Applied Mechanics* (under review). Finite element transient response of composite and sandwich plates with a refined higher-order theory.
32. R. M. JONES 1975 *Mechanics of Composite Materials*. New York: McGraw-Hill.
33. K. J. BATHE 1982 *Finite Element Procedures in Engineering Analysis*. Englewood Cliffs, New Jersey: Prentice-Hall.
34. E. HINTON, T. ROCK and O. C. ZIENKIEWICZ 1976 *Earthquake Engineering and Structural Dynamics* 4, 245–249. A note on mass lumping and related processes in the finite element method.
35. A. K. GUPTA and A. MOHRAZ 1972 *International Journal of Numerical Methods in Engineering* 5, 83–92. A method of computing numerically integrated stiffness matrices.
36. MALLIKARJUNA and T. KANT 1989 *International Journal for Numerical Methods in Engineering* (in press). Free vibration of symmetrically laminated plates using a refined higher-order theory with finite element technique.

APPENDIX A

The rigidity matrices $\underset{\sim}{D}_m$, $\underset{\sim}{D}_c$, $\underset{\sim}{D}_b$ and $\underset{\sim}{D}_s$ are as follows.

$$\underset{\sim}{D}_m = \sum_{L=1}^{n} \begin{bmatrix} Q_{11}H_1 & Q_{12}H_1 & Q_{14}H_1 & Q_{11}H_3 & Q_{12}H_3 & Q_{14}H_3 & Q_{13}H_1 \\ & Q_{22}H_1 & Q_{24}H_1 & Q_{12}H_3 & Q_{22}H_3 & Q_{24}H_3 & Q_{23}H_1 \\ & & Q_{44}H_1 & Q_{14}H_3 & Q_{24}H_3 & Q_{44}H_3 & Q_{34}H_1 \\ & & & Q_{11}H_5 & Q_{12}H_5 & Q_{14}H_5 & Q_{13}H_3 \\ & & & & Q_{22}H_5 & Q_{24}H_5 & Q_{23}H_3 \\ & & & & & Q_{44}H_5 & Q_{34}H_3 \\ & & & & & & Q_{33}H_1 \end{bmatrix}^{L\text{th layer}} . \tag{A1}$$

The matrix $\underset{\sim}{D}_c$ can be obtained by replacing H_1, H_3 and H_5 by H_2, H_4 and H_6 respectively in the above matrix $\underset{\sim}{D}_m$. Similarly, the matrix $\underset{\sim}{D}_b$ can be obtained by replacing H_1, H_3 and H_5 by H_3, H_5 and H_7 respectively in the above matrix $\underset{\sim}{D}_m$.

$$\underset{\sim}{D}_s = \sum_{L=1}^{n} \begin{bmatrix} Q_{66}H_1 & Q_{65}H_1 & Q_{66}H_2 & Q_{65}H_2 & Q_{66}H_3 & Q_{65}H_3 \\ & Q_{55}H_1 & Q_{56}H_2 & Q_{55}H_2 & Q_{56}H_3 & Q_{55}H_3 \\ & & Q_{66}H_3 & Q_{65}H_3 & Q_{66}H_4 & Q_{65}H_4 \\ & & & Q_{55}H_3 & Q_{56}H_4 & Q_{55}H_4 \\ & & & & Q_{66}H_5 & Q_{65}H_5 \\ & & & & & Q_{55}H_5 \end{bmatrix}^{L\text{th layer}} . \tag{A2}$$

In all the above relations, n is the number of layers and

$$H_i = (1/i)(h^i_{L+1} - H^i_L), \qquad i = 1, 2, \ldots, 7.$$